

Journal of Materials Chemistry A

Accepted Manuscript



This is an *Accepted Manuscript*, which has been through the Royal Society of Chemistry peer review process and has been accepted for publication.

Accepted Manuscripts are published online shortly after acceptance, before technical editing, formatting and proof reading. Using this free service, authors can make their results available to the community, in citable form, before we publish the edited article. We will replace this *Accepted Manuscript* with the edited and formatted *Advance Article* as soon as it is available.

You can find more information about *Accepted Manuscripts* in the [Information for Authors](#).

Please note that technical editing may introduce minor changes to the text and/or graphics, which may alter content. The journal's standard [Terms & Conditions](#) and the [Ethical guidelines](#) still apply. In no event shall the Royal Society of Chemistry be held responsible for any errors or omissions in this *Accepted Manuscript* or any consequences arising from the use of any information it contains.



Journal Name

ARTICLE

Room-Temperature Driven and Visible Light Enhanced Dehydrogenation Reactions Catalysed by Basic Au/SrTiO₃

Huimin Liu^a, Tao Wang^a, Huabin Zhang^a, Guigao Liu^{a,b}, Peng Li^a, Lequan Liu^c, Dong Hao^a, Jian Ren^c, Kun Chang^a, Xianguang Meng^a, Hongmei Wang^c and Jinhua Ye^{a,b,c,d*}

Received 00th January 20xx,
Accepted 00th January 20xx

DOI: 10.1039/x0xx00000x

www.rsc.org/

Au/SrTiO₃ catalyst with basic property (Au/SrTiO₃-urea) was firstly reported to be efficient for the dehydrogenation of secondary alcohols at room temperature, with iso-propanol (IPA) dehydrogenation as the probe reaction. Different from previous reports that Au/SrTiO₃ was generally regarded as only photocatalyst in IPA dehydrogenation reaction, in this work, it was found that Au/SrTiO₃-urea could also catalyse the reaction at room temperature without light irradiation, with an acetone production rate of 8.2 μmol·h⁻¹ (IPA conversion 41.0 %) which was more than 10 times higher than that of Pt/TiO₂ evaluated under the same conditions. Characterization results revealed that the lattice oxygen on SrTiO₃ was involved in the reaction through the Mars-van Krevelen mechanism, while Au facilitated the cleavage of C-H bond of the adsorbed reactant with the assistance of base. Its catalytic activity was further increased to 16.5 μmol·h⁻¹ (IPA conversion 82.5 %) after the introduction of visible light. It's regarded that the photon induced photocatalytic performance was significantly enhanced with the existence of instantaneously generated oxygen vacancies. Additionally, the conversion of IPA (82.5%) and the rate of acetone production over Au/SrTiO₃-urea (16.5 μmol·h⁻¹) after visible light irradiation for 1 h were 12.3 times and 2.5 times as high as those over Au/P25 (IPA conversion of 6.7 % and acetone production rate of 6.7 μmol·h⁻¹), a catalyst which was also reported to exhibit somewhat activity in IPA dehydrogenation without light irradiation. This study provides a method for designing efficient catalysts for the dehydrogenation of secondary alcohols at room temperature.

1. Introduction

Due to the relentless environmental concerns and risky demands for the fossil fuels, iso-propanol (IPA) dehydrogenation has overwhelmed the other methods (such as Wacker oxidation [1] and Cumene process [2]) and become the most economical one for acetone generation [3-4]. Previously, thermal catalytically converting IPA is the primary avenue, and acetone could be produced on platinum (Pt) or palladium (Pd) based catalysts at low temperatures whereas Pt and Pd were not stable to oxidation [5]. Many other metal based catalysts could also convert IPA to acetone, however relatively high temperatures were required (>100 °C) [3-4]. Since the entry of the photocatalysis era milestone by the water splitting over TiO₂ catalyst [6], utilizing the abundant solar energy, especially visible light [7], to dehydrogenate IPA to acetone has

attracted the attentions of scientists [8-9]. Semiconductors [8] and metals with local surface plasmon resonance (LSPR) [9-10] could be used as photocatalysts in IPA dehydrogenation without external heat supply, however the rate of acetone generation was limited due to the low energy utilization efficiency [11-14]. Therefore, to efficiently dehydrogenate IPA to acetone at room temperature, it's critically important to develop a photo-catalytically active catalyst that also works effectually at low temperatures (Thermodynamic study is shown in the Supporting Information).

To the best of our knowledge, there was only one photocatalyst which also exhibited somewhat activity in IPA dehydrogenation without light irradiation [15], and it is Au/P25 with gold nanoparticles located at the interface of anatase/rutile TiO₂. However, the activity of the Au/P25 catalyst evaluated under dark condition was not high, only about 1.7 μmol·h⁻¹ [15], and the reason for the activity was not discussed. For this reason, it's urgently needed to enhance the performance of a catalyst at room temperature without light irradiation and study the mechanism in detail with the aim to provide theoretical guidance for further improvement.

From the kinetic point of view, depending on the catalyst employed, the rate determining step of the IPA dehydrogenation reaction fits into the following two different patterns: (1) cleavage of C-H bond of adsorbed IPA species and (2) the rate of oxygen transport to the catalyst surface [5]. To enhance the cleavage of C-H bond, Au was selected as the active component of the catalysts in this work, since Au was one of the metals reported to be favourable

^a Environmental Remediation Materials Unit, International Center for Materials Nanoarchitectonics (WPI-MANA), National Institute for Materials Science (NIMS), 1-1 Namiki, Tsukuba, Ibaraki 305-0044, Japan

^b Graduate School of Chemical Science and Engineering, Hokkaido University, Sapporo 060-0814, Japan

^c TU-NIMS Joint Research Center, School of Materials Science and Engineering, Tianjin University, 92 Weijin Road, Nankai District, Tianjin 300072, China

^d Collaborative Innovation Center of Chemical Science and Engineering (Tianjin), Tianjin 300072, China

* Corresponding author, jinhua.ye@nims.go.jp, Tel: +81-29-859-2646 Fax: +81-29-859-2301

Electronic Supplementary Information (ESI) available: [details of any supplementary information available should be included here]. See DOI: 10.1039/x0xx00000x

both in breaking C-H bond [16-17] and in photocatalytic reactions owing to LSPR [8-9]. About the issue on oxygen transport, employing supports with active lattice oxygen might be a solution. For redox reactions with O₂ as one of the reactants, the lattice oxygen in the catalysts might be involved through the Mars-van Krevelen mechanism [18] and the reaction rate hindered by oxygen transfer could be improved significantly. Among the semiconductors widely employed in photocatalysis, SrTiO₃ was supposed to be promising as support owing to that the oxygen in its lattice structure could be partially isotope exchanged at low temperatures [19-20]. For the above mentioned two reasons, Au/SrTiO₃ was expected to be efficient both as photocatalyst and thermal catalyst for IPA dehydrogenation. However, there were no reports about the utilization of Au/SrTiO₃ in the degradation of VOCs (volatile organic compounds) at room temperature without light irradiation, and the results in Fig. S1 also revealed that Au/SrTiO₃ prepared by photoreduction method with methanol as reductant exhibited nearly no activity in IPA dehydrogenation without light illumination. Considering the fact that base is needed to activate the reactants when Au-based catalysts were employed for aerobic oxidation of alcohols [21], in this paper, Au/SrTiO₃ catalyst of basic property was synthesized with the expectation to be superior in IPA dehydrogenation, and the influences of basicity, lattice oxygen and plasmonic Au were investigated in detail.

2. Experimental

2.1 Catalyst preparation

Commercial anatase TiO₂, SrTiO₃, HAuCl₄, CH₃OH and CO(NH₂)₂ were purchased from Wako pure chemical industries Ltd and used as raw materials.

Preparation of Au/SrTiO₃ and Au/SrTiO₃-urea: Gold was loaded on SrTiO₃ via urea precipitation method. A 1.0 g portion of SrTiO₃ (purity>99.9%) was added into 100 mL aqueous solution of urea (purity>99.0%, 11.4 g) and HAuCl₄ (purity>99.0%). The suspension was treated at 80 °C for 4 h with vigorous stir, and then separated into two equal parts. One was washed with excessive amount of deionized water until pH=7, dried, and calcined at 400 °C for 4 h, and the obtained sample was denoted as Au/SrTiO₃. Another part was washed with 500 mL of deionized water (with a certain amount of urea residual), dried, and calcined at 400 °C for 4 h, and the obtained sample was denoted as Au/SrTiO₃-urea. The theoretical loading of Au was 2 wt.%.

Preparation of Au/TiO₂ and Au/TiO₂-urea: The preparation procedures of Au/TiO₂ and Au/TiO₂-urea were the same as those of Au/SrTiO₃ and Au/SrTiO₃-urea, except that TiO₂ (purity>99.9%) instead of SrTiO₃ was employed as support.

Preparation of the reference catalysts: As reference, Au/SrTiO₃ was also synthesized by photoreduction method with CH₃OH (purity>99.5%) as the reductant. Pt/TiO₂ was also prepared by photoreduction method with CH₃OH as the reductant. In the paper, unless otherwise stated, Au/SrTiO₃ was referred to the catalyst with Au loaded via the urea precipitation method.

2.2 Material characterization

The crystalline structures of the supports and Au-based catalysts were analysed by X-ray diffraction (XRD) method, on an X-

Pert diffractometer equipped with graphite monochromatized Cu-K α radiation. The specific surface areas were determined with a surface area analyser (BEL Sorp-II mini, BEL Japan Co., Japan) by the Brunauer-Emmett-Teller (BET) method. The morphology and the sizes of Au particles were observed on transmission electron microscope JEM-2100 (TEM, JEOL, USA). The diffuse reflection spectra of the catalysts were measured by UV-Vis spectrophotometer (UV-2600, SHIMADZU Co., Japan) from 200 nm to 800 nm. The contents of Au on the catalysts were analysed by inductively coupled plasma optical emission spectrometry (ICP-OES, SPS3520UV-DD, SII nano technology Inc., Japan). The oxygen vacancies were analysed by electron spin resonance (ESR) on JEOL JES-FA-200. The basic properties of the catalysts were characterized by CO₂ temperature programmed desorption method (CO₂-TPD, Autochem II 2920). The decomposition behaviour of the Au/SrTiO₃-urea catalyst was studied by thermogravimetric analysis method (TGA, DTA-60H, Shimadzu) and O₂ temperature programmed decomposition method (O₂-TPD, Autochem II 2920). The photocurrents of the catalysts were performed on the CHI electrochemical analyser (ALS/CH model 650A) using a standard three-electrode mode with 0.5 M Na₂SO₄ solution as the electrolyte. For the photocurrent analysis, HA30 and L42 cut-off filters were employed to remove ultraviolet and infrared light.

2.3 Catalyst evaluation

In a typical IPA dehydrogenation reaction, 0.15 g catalyst was uniformly dispersed on the bottom surface of a vessel (5.6 cm²) which was placed in a glass reaction cell of 500 mL. The catalyst temperature was probed by a digital thermometer (CT-1200D, CUSTOM Co., Japan). The cell was totally covered by tinfoil and then IPA was injected into the cell through an installed inlet/outlet port. For the reaction carried out at room temperature without light illumination, 30 min was required to ensure the adsorption-desorption equilibrium of the gaseous reactants. After that the concentrations of IPA, acetone, and CO₂ were measured using a gas chromatograph (GC-14B, Shimadzu) equipped with a flame ionization detector (FID). Porapak Q and PEG-1000 columns were used to detect CO₂ and the two organic gases (IPA and acetone), respectively. Isotope experiment was also conducted with ¹⁸O₂ and IPA as the reactants, with the labelled products analysed by gas chromatography-mass spectrometry (GC-MS, JMS-K9, JEOL Co., Japan). As to IPA dehydrogenation with visible light irradiation, HA30 and L42 cut-off filters were employed to remove ultraviolet and infrared light. The reaction cell was also kept in dark for 30 min before turning on the 300 W Xe arc lamp.

3. Results and discussion

3.1 Physicochemical properties of the supports and catalysts

The crystalline structures of the prepared catalysts were characterized by XRD, with the results shown in Fig. 1a. Clearly, TiO₂ and SrTiO₃ exhibited their own typical diffraction peaks on the XRD profiles, and the urea treated supports and the relevant Au-based catalysts demonstrated only the peaks attributed to the support whereas no obvious peaks assigned to Au were observed (the existence of Au was analysed by ICP-OES, in Table S1, and in the range of 1.9~2.6 wt.%, close to theoretical values), indicating the

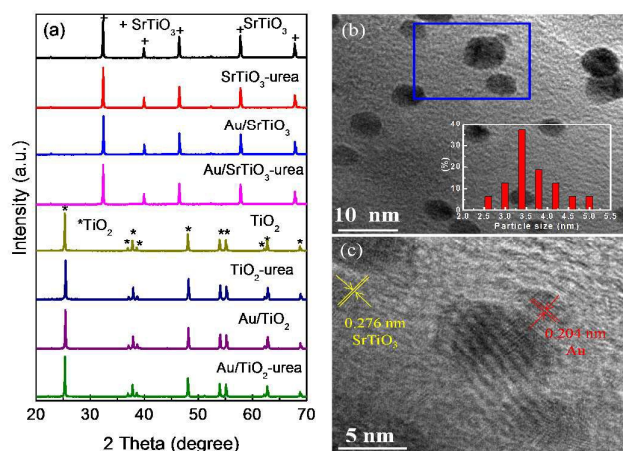


Fig. 1 (a) XRD patterns of SrTiO₃, TiO₂ and their supported catalysts, (b) TEM images of Au/SrTiO₃-urea with Au size distribution as the inset, and (c) HRTEM images of Au/SrTiO₃-urea (the square part of Fig. 1b).

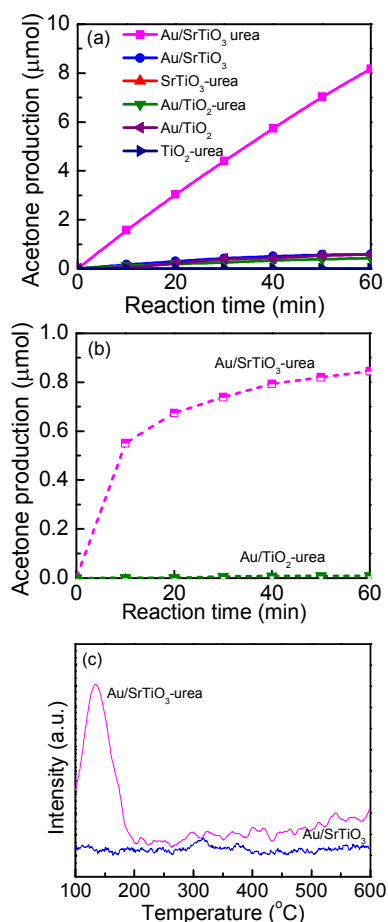


Fig. 2 (a) Catalytic performances of the supports and catalysts in IPA dehydrogenation under dark conditions, (b) Catalytic performances of Au/SrTiO₃-urea and Au/TiO₂-urea evaluated under vacuum condition, and (c) CO₂-TPD profiles of Au/SrTiO₃-urea and Au/SrTiO₃. Reaction conditions: catalyst 0.15 g, initial IPA 20 μmol, room temperature (23 °C), without light irradiation.

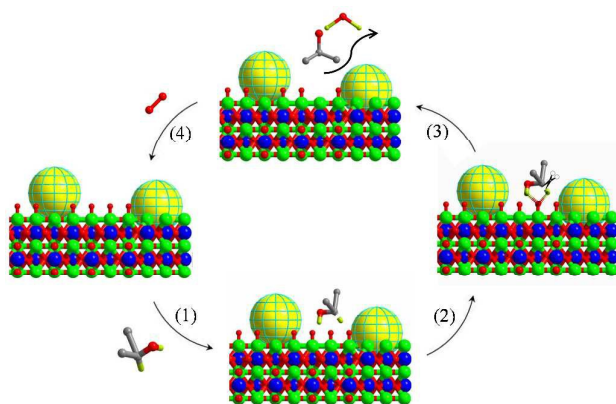
Au particles were quite small and well dispersed. TEM images of Au/SrTiO₃-urea and Au/SrTiO₃, displayed in Fig. 1b, 1c and Fig. S2 delivered consistent information with that of XRD patterns. Small spherical Au particles, 2~5 nm (the inset of Fig. 1b and Fig. S2), were dispersed uniformly on the support (TEM and HRTEM images in Fig. 1b and Fig. 1c, respectively). The specific surface areas of the supports and catalysts were analysed through N₂ adsorption-desorption isotherms (Fig. S3) and calculated via Brunauer-Emmett-Teller (BET) equation, and in the range of 1~2 m² g⁻¹ for the SrTiO₃ related samples and 6~8 m² g⁻¹ for the TiO₂ related ones (Table S1), which implied that the urea treatment and the loading of Au affected little on the surface area of the catalysts.

3.2 Catalytic performance of the catalysts under dark conditions

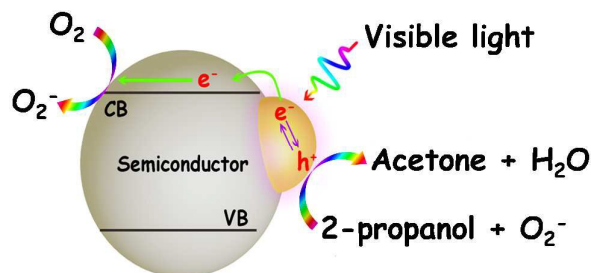
The catalytic performances of the catalysts in IPA dehydrogenation without light irradiation were evaluated at optimized conditions (Fig. S4) with the results in Fig. 2a. Noticeably, Au/SrTiO₃-urea presented a high catalytic activity in IPA dehydrogenation to acetone (8.2 μmol acetone generated within 1 h, 41.0% IPA conversion, which was more than 10 times higher than that over Pt/TiO₂ in Fig. S5), and since IPA dehydrogenation reaction is first order with IPA concentration (Fig. S4), IPA conversion will remain constant with the further increase of initial IPA concentrations, and increase with reaction temperature (Fig. S6) and catalyst dosage (Fig. S7). In sharp contrast, all the other reference catalysts or supports (including SrTiO₃ and TiO₂) exhibited negligible performances (Fig. 2a). The catalytic performance differences between Au/SrTiO₃-urea and Au/TiO₂-urea (Fig. 2a) might be related with the involvement of lattice oxygen (SrTiO₃ and TiO₂ are oxygen containing compound, thus there are lattice oxygen in their lattice structures definitely), since the lattice oxygen in SrTiO₃ could easily involve in a redox reaction at room temperature [18-19], on the other hand, only about 3.3 % of the lattice oxygen on TiO₂ surface can be extracted from its lattice structure at 400 °C [22]. To check whether the lattice oxygen was involved in the reaction, IPA dehydrogenation was carried out in oxygen deficient atmosphere (Fig. 2b). Obviously, no activity was observed on Au/TiO₂-urea, whereas over Au/SrTiO₃-urea catalyst, it's amazing to note that acetone could be formed even without the existence of O₂ and no H₂ was detected, suggesting that H₂O was the byproduct with the O atom in H₂O coming from the support via the Mars-van Krevelen mechanism. Isotope labelling experiment with ¹⁸O₂ as the reactant was adopted to further ascertain the involvement of lattice oxygen, with the results displayed in Fig. S8. Apparently, both H₂¹⁶O and H₂¹⁸O were detected as the byproducts (and no ¹⁸O labelled acetone could be detected), which implied that both the gaseous ¹⁸O₂ and the lattice oxygen ¹⁶O in SrTiO₃ were participated in the formation of water. Both of the two above results elucidated the indispensable effect of lattice oxygen in the reaction occurrence.

However, lattice oxygen was not the only reason for the excellent performance of Au/SrTiO₃-urea at room temperature without light illumination, since Au/SrTiO₃ did not show any potential in IPA decomposition, which clarified that the trace amount of residual urea during the washing process also played an important role in the catalyst design. The mass balances were calculated over Au/SrTiO₃-urea catalysts, in the range of 99.8 ~ 102.9% (Table S2), indicating the acetone formed was originated

from IPA not from the residual urea. The decomposition behaviour of Au/SrTiO₃-urea was studied via O₂-TPD (in Fig. S9) and TGA (in Fig.



Scheme 1 Possible mechanism for IPA dehydrogenation at room temperature without light irradiation.



Scheme 2 Possible mechanism of Au-based photocatalysts in IPA dehydrogenation.

S10), which suggested that the residual urea during washing process was totally decomposed in the following calcination process. CO₂-TPD was carried out to investigate the intrinsic influences of the residual urea, and the results are shown in Fig. 2c. There was a sharp peak due to CO₂ desorption over Au/SrTiO₃-urea, which implied that Au/SrTiO₃-urea was a catalyst with basic sites whereas Au/SrTiO₃ was not. Earlier reports disclosed that basic sites would be formed (O was partially substituted by N) after treating a material with ammonia at high temperature [23-24]. In this case, the basicity over Au/SrTiO₃-urea could be assigned to the treatment with ammonia, which was generated by the decomposition of urea during the catalyst calcination process. On the contrary, the electronic structures of Au and SrTiO₃ were not influenced greatly due to that the amount of N substitution was quite small (Fig. S11). The basic sites of a catalyst were reported to be requisite in promoting alcohol adsorption [21].

The sharp contrast between the performances of SrTiO₃-urea and Au/SrTiO₃-urea (Fig. 2a) revealed coincident results with the previous reports that Au participated in facilitating and activating the cleavage of C-H bond [16-17]. Then the mechanism of IPA dehydrogenation over the Au-based catalysts at room temperature without light illumination could be illustrated in Scheme 1. IPA was firstly adsorbed on the surface lattice oxygen of the support SrTiO₃ with the assistance of base, and acetone could be formed with the

neighbouring Au particles breaking the C-H bond of the adsorbed IPA species, and then the oxygen vacancy formed would be occupied soon by the atmospheric air (Scheme 1). This mechanism was also compliant to the dehydrogenation of other secondary alcohols, such as 2-butanol and 2-pentanol (Fig. S12).

3.3 Catalytic performance of the catalysts with visible light irradiation

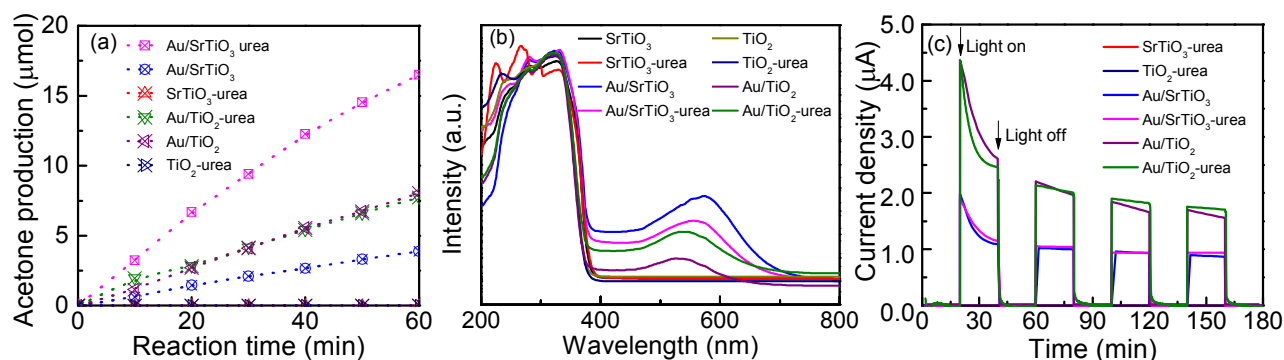
Au/SrTiO₃ and Au/TiO₂ was also widely studied in photocatalytic reactions owing to the semiconductor properties of SrTiO₃ or TiO₂ and the LSPR characteristics of Au [9-10, 15]. The catalytic performances of the catalysts in IPA dehydrogenation with visible light irradiation were evaluated with the results displayed in Fig. 3a. Apparently, except the support SrTiO₃, TiO₂ and the urea treated ones, all the other four Au-based catalysts exhibited enhanced performances (Fig. 3a) compared with those obtained without light irradiation (Fig. 2a). For Au/SrTiO₃, Au/TiO₂ and Au/TiO₂-urea catalysts, since nearly no catalytic activities were observed in IPA dehydrogenation without light irradiation (Fig. 2a), their enhanced performances under light irradiation could be totally ascribed to the photon induced photocatalytic activities (Fig. 3a) [9-10].

UV-visible spectra of the supports and catalysts in Fig. 3b revealed that the supports could not absorb visible light, whereas the Au-based catalysts exhibited the typical absorption peaks attributed to spherical Au LSPR in the range of 520~560 nm [9-10]. The band gaps of SrTiO₃ and TiO₂ over the relevant samples were calculated to be 3.2 eV and 3.3 eV, respectively, which conformed to the previous results within detection errors [25-26]. Together with the Mott-Schottky plots in Fig. S10, the valence band and conduction band of the catalysts could be calculated and obtained (Table S3). The conduction band of SrTiO₃ and TiO₂ related samples was -0.2 eV and -0.4 eV (Table S3), respectively. The hot electrons generated on Au nanoparticles under visible light irradiation could be transferred to the conduction band of the semiconductor [27-28], which was confirmed by the significantly higher photocurrent over Au-based catalyst (Fig. 3c). According to the information above and previous reports [9, 27-28], the mechanism of the three Au-based catalysts in photocatalytic IPA dehydrogenation could be proposed as displayed in Scheme 2. With the irradiation of visible light, Au LSPR could be excited with electrons and holes being generated and separated, then the electron would transfer to the conduction band of the support (SrTiO₃ or TiO₂) [27-28] and lead to the formation of superoxide (O₂⁻) [29-30]. The superoxide is of strong oxidizing property and can oxidize IPA to acetone [31] by giving one electron to Au particle.

The catalytic performances over Au/SrTiO₃, Au/TiO₂ and Au/TiO₂-urea in IPA dehydrogenation under visible light irradiation were ascribed to the photon induced photocatalytic activities. Then what about the case over Au/SrTiO₃-urea catalyst? Considering the facts that the trace amount of urea residual during the washing process didn't affect the conduction band and valence band (analysed by UV-visible spectra in Fig. 3b and Mott-Schottky plots in Fig. S13), the photocurrents (Fig. 3c) and the catalytic performances under visible light irradiation (Fig. 3a), the photon induced photocatalytic activity over Au/SrTiO₃-urea could be assumed to be the same as that of Au/SrTiO₃. Notably, the catalytic activity of Au/SrTiO₃-urea under visible light was much higher than the sum of

the performances of Au/SrTiO₃-urea evaluated without light irradiation and Au/SrTiO₃ under visible light irradiation, which gave evidences that there might be other reasons for the greatly enhanced performance of Au/SrTiO₃-urea in IPA dehydrogenation

Nano-architectonics (MANA), MEXT (Japan), the National Basic Research Program of China (973 Program, 2014CB239301) and the Mitsubishi Foundation.



with visible light irradiation. In consideration of the earlier reports Fig.3 (a) catalytic performance of the supports and catalysts in IPA dehydrogenation under visible light irradiation, (b) UV-visible spectra of the supports and catalysts, and (c) Current density of the supports and catalysts under visible light irradiation.

Reaction conditions: catalyst 0.15 g, initial IPA 20 μmol, room temperature (23 °C), visible light irradiation (L42 and HA30 as filters).

that oxygen vacancies could effectively influence light absorption and improve the catalytic performance of a photocatalyst with light irradiation [32], in this case, the instantaneous generated oxygen vacancies, even though they would be soon occupied by the atmospheric oxygen (*in-situ* ESR results in Fig. S14 and XRD patterns in Fig. S15), might play an important role in enhancing the photocatalytic activity of Au/SrTiO₃-urea.

4. Conclusions

In summary, this study offers a research tactic for preparing effective Au-based catalysts in IPA dehydrogenation at room temperature, no matter with or without light irradiation. Without light irradiation, SrTiO₃ as support supplies the active lattice oxygen for the adsorption of IPA with the assistance of base, and Au particles possess the ability to cleavage the C-H bond of the adsorbed IPA, and the rate of acetone production over the Au/SrTiO₃-urea catalyst was 8.2 μmol·h⁻¹ (IPA conversion was 41.0 %), 10 times higher than that over Pt/TiO₂. With the irradiation of visible light, the photon induced photocatalytic performance was significantly enhanced with the existence of instantaneously generated oxygen vacancies, which further improved the catalytic activity of Au/SrTiO₃-urea to 82.5% IPA conversion and 16.5 μmol·h⁻¹ acetone production rate. The preparation strategy of the Au-based catalysts was forecasted to be applicable for the dehydrogenation of versatile secondary alcohols at room temperature.

Acknowledgements

This work received financial support from the World Premier International Research Center Initiative (WPI Initiative) on Materials

Notes and references

- G. P. Chiusoli and P. M. Maitlis, *Royal Society of Chemistry*, 2008, pp 69-70.
- G. D. Yadav and N. S. Asthana, *Appl. Catal. A: Gen.*, 2003, **244**, 341.
- R. M. Rioux and M. A. Vannice, *J. Catal.*, 2003, **216**, 362.
- H. Cao and S. L. Suib, *J. Am. Chem. Soc.*, 1994, **116**, 5334.
- J. W. Nicoletti and G. M. Whitesides, *J. Phys. Chem.*, 1989, **93**, 159.
- A. Fujishima and K. Honda, *Nature*, 1972, **238**, 37.
- Z. Zou, J. Ye, K. Sayama and H. Arakawa, *Nature*, 2001, **414**, 625.
- D. Chen, S. Ouyang and J. Ye, *Nanoscale Res. Lett.*, 2009, **4**, 274.
- L. Liu, T. D. Dao, R. Kodiyath, Q. Kang, H. Abe, T. Nagao and J. Ye, *Adv. Funct. Mater.*, 2014, **24**, 7754.
- L. Liu, S. Ouyang and J. Ye, *Angew. Chem. Int. Ed.*, 2013, **52**, 6689.
- M. Ni, M. K. H. Leung, D. Y. C. Leung and K. Sumathy, *Renew. Sust. Energ. Rev.*, 2007, **11**, 401.
- S. Ouyang and J. Ye, *J. Am. Chem. Soc.*, 2011, **133**, 7757.
- H. Liu, X. Meng, T. D. Dao, H. Zhang, P. Li, K. Chang, T. Wang, M. Li, T. Nagao and J. Ye, *Angew. Chem. Int. Ed.*, 2015, **54**, 11545.
- H. Liu, H. Zhang, L. Shi, X. Hai and J. Ye, *Appl. Catal. A: Gen.*, 2015, doi:10.1016/j.apcata.2015.10.027.
- D. Tsukamoto, Y. Shiraishi, Y. Sugano, S. Ichikawa, S. Tanaka and T. Hirai, *J. Am. Chem. Soc.*, 2012, **134**, 6309.
- C. Wei and C. Li, *J. Am. Chem. Soc.*, 2003, **125**, 9584.
- M. Jiang, L. Liu, M. Shi and Y. Li, *Org. Lett.*, 2010, **12**, 116.
- A. M. Ali, E. A. C. Emanuelsson and D. A. Patterson, *Appl. Catal. B: Environ.*, 2010, **97**, 168.
- S. Ferrer and G. A. Somorjai, *Surf. Sci.*, 1980, **97**, L304.
- M. Itoh and R. Wang, *Appl. Phys. Lett.*, 2000, **76**, 221.
- P. Liu, Y. Guan, R. A. van Santen, C. Li and E. J. M. Hensen, *Chem. Commun.*, 2011, **47**, 11540.
- D. Widmann and R. J. Behm, *Angew. Chem. Int. Ed.*, 2011, **50**, 10241.
- S. Sahin, P. Mäki-Arvela, J. P. Tessonnier, A. Villa, L. Shao, D. S. Su, R. Schlögl, T. Salmi and D. Y. Murzin, *Stud. Surf. Sci. Catal.*, 2010, **175**, 283.
- J. Przepiorski, M. Skrodziewicz and A. W. Morawski, *Appl. Surf. Sci.*, 2004, **225**, 235.

ARTICLE

Journal Name

- 25 K. V. Benthem, C. Elsässer and R. H. French, *J. Appl. Phys.*, 2001, **90**, 6156.
- 26 S. U. M. Khan, M. Al-Shahry and W. B. I. Jr., *Science*, 2002, **297**, 2243.
- 27 S. Linic, P. Christopher and D. B. Ingram, *Nat. Mater.*, 2011, **10**, 911.
- 28 A. Furube, L. Du, K. Hara, R. Katoh and M. Tachiya, *J. Am. Chem. Soc.*, 2007, **129**, 14852.
- 29 T. Hirakawa and Y. Nosaka, *J. Phys. Chem. C*, 2008, **112**, 15818.
- 30 Y. Chen, A. Lu, Y. Li, L. Zhang, H. Y. Yip, H. Zhao, T. An and P. Wong, *Environ. Sci. Technol.*, 2011, **45**, 5689.
- 31 V. Iliev, *J. Photoch. Photobio. A*, 2002, **151**, 195.
- 32 I. Nakamura, N. Negishi, S. Kutsuna, T. Ihara, S. Sugihara and K. Takeuchi, *J. Mol. Catal. A*, 2000, **161**, 205.

